Transient Analysis Method for Plasmonic Devices by PMCHWT With Fast Inverse Laplace Transform

Seiya Kishimoto, Shao Ying Huang, *Member, IEEE*, Yoshito Ashizawa, *Member, IEEE*, Katsuji Nakagawa, *Member, IEEE*, Shinichiro Ohnuki, *Member, IEEE*, and Weng Cho Chew, *Fellow, IEEE*

***Abstract*—The transient analysis of electromagnetic problems is important in the designing of plasmonic devices. It is useful for clarifying physical phenomena with extremely short timescales, because transient response affects the device performance. A time-domain computational technique is proposed for the transient analysis of electromagnetic problems with nanostructures. Our method is based on boundary integral equations in the complex frequency domain and fast inverse Laplace transforms. The advantage of our method is that the objects can be modeled by surface structure, dispersive media can be easily considered, computational error analysis is simple, and the electromagnetic field at the desired observation time can be obtained.**

***Index Terms*—Fast inverse Laplace transform (FILT), plasmonic device, Poggio–Miller–Chang–Harrington–Wu–Tsai (PMCHWT), transient analysis.**

I. Introduction

RECENTLY, a helicity-dependent all-optical magnetic switching has attracted attention for ultrafast magnetic recording systems [1]–[3]. The recording speed of this system is 100 000× faster than conventional magnetic recording systems. It is a requirement for imping circular polarized light for magnetic reversal. Furthermore, the localized light is necessary because the magnetic recording density is related to the beam spot size. To realize these requirements, a plasmonic antenna is designed as the localized light can be beyond the diffraction limit [4]–[6]. Although many plasmonic devices are designed using properties based on frequency response, it is important to investigate the characteristics of transient response in the helicity-dependent all-optical magnetic switching. The recording speed is related to the transient state of light.

Manuscript received January 24, 2022; accepted February 19, 2022. Date of publication February 23, 2022; date of current version May 5, 2022. This work was supported by in part by JSPS KAKENHI under Grant JP21K17753 and in part by a research grant from the College of Science and Technology, Nihon University. *(Corresponding author: Seiya Kishimoto.)*

Seiya Kishimoto, Yoshito Ashizawa, Katsuji Nakagawa, and Shinichiro Ohnuki are with the College of Science and Technology, Nihon University, Tokyo 101-8308, Japan (e-mail: kishimoto.seiya@nihon-u.ac.jp; ashizawa.yoshito@nihon-u.ac.jp; nakagawa.katsuji@nihon-u.ac.jp; ohnuki.shinichiro@nihon-u.ac.jp).

Shao Ying Huang is with the Engineering Product Development, Singapore University of Technology and Design, Singapore 487372 (e-mail: huangshaoying@sutd.edu.sg).

Weng Cho Chew is with the School of Electrical and Computer Engineering, Purdue University, West Lafayette, IN 47907 USA (e-mail: wcchew@purdue.edu).

Digital Object Identifier 10.1109/LAWP.2022.3153650

Conventionally, the finite-difference time-domain (FDTD) method is used for studying these plasmonic devices [7]. However, since metal is dispersive in the optical frequency band, it is difficult to implement with FDTD. Furthermore, when considering the fine structure, the minimum discretized segmented area, which is the cell size for FDTD, is very small. The stability condition of the explicit FDTD becomes strict. The time step size depends on the minimum cell size, so the computational time increases for more accurate computation.

Previously, we proposed the novel computational method as an alternative technique to FDTD for designing plasmonic devices. Maxwell's equations are solved by the finite-difference complex-frequency-domain method [8]–[10]. The solution in the complex frequency domain is transformed into the time domain using a fast inverse Laplace transform (FILT) [11]–[13]. The advantages of this method are the following: the dispersive media is easy to implement, computational modeling is compatible with FDTD, and it is suitable for the parallel computation [10]. However, it is necessary to implement an absorption boundary. Moreover, when staircase approximation same as FDTD is used for modeling, a singular phenomenon occurs on the surface of the object that causes computational errors in near-field analysis.

In this letter, a novel transient computational technique for analysis of the nanoscale electromagnetic problems is proposed. Our method has the following advantages: dispersive media can be easily considered, the absorption boundary condition is not necessary, and the objects can be modeled by only the surface structure. The boundary integral equation method is applied for solving the complex frequency domain problems. Here, Poggio–Miller–Chang–Harrington–Wu–Tsai (PMCHWT) is used for integral equation and extended in the complex frequency domain [14]. The electromagnetic field at the observation time can be obtained by using FILT [11]. FILT is error controllable method, thus, computational error analysis is simple. The solution at the desired observation time can be obtained. Furthermore, time-division parallel computing can be easily realized [9], [10].

These advantages are suitable for designing plasmonic devices where evaluation of the time response is important. To demonstrate our method, the plasmonic antenna for helicity-dependent all-optical magnetic switching has been designed. The investigation of steady-state and transient-state responses are evaluated to confirm that generation of high-intensity circularly polarized light and the stability of magnetization switching speed, respectively. Compared with the time-domain PMCHWT,

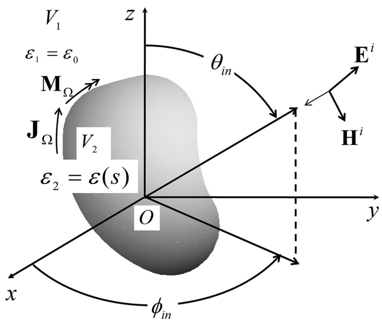

Fig. 1. Geometry and coordinates systems.

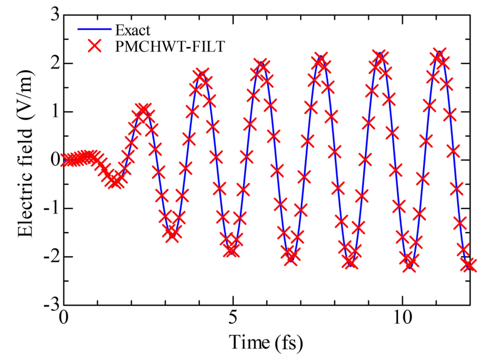

Fig. 2. Time-domain responses of the electric field near a gold nano sphere with a 25 nm radius.

the proposed method has advantages as follows. 1) The electromagnetic fields can be independently evaluated at the specific desired time. 2) The dispersive medium can be treated in the same implementation as in the frequency domain [15], [16]. Also, compared with inverse fast Fourier transform based methods, our proposed method is more appropriate and efficient especially for plasmonic antenna design [17]. When the electromagnetic field rapidly changes in time, computation using the unequal and coarse sampling values in time domain is useful for brief and quick estimation. Sampling points can be later added by using our technique when detailed evaluation is needed.

II. Formulation

The scatterer is a metallic nano object, as shown in Fig. 1. The electromagnetic fields $\mathbf{E}^i$ and $\mathbf{H}^i$ impinge on the scatterer to form incident angles θ_{in} and ϕ_{in}. The time-domain waveform of the incident wave is expressed as the image function of $\hat{f}(s)$. Here, $s = \sigma + i\omega$ is complex frequency, σ is a real number, and ω is real frequency. The permittivity of the object is ε_2 and has dispersive characteristics $\varepsilon(s)$. The Lorentz–Drude model is extended in the complex frequency domain for the expression of metal properties [18].

The boundary integral equation for homogeneous media, which is PMCHWT formulation, is expressed with the equivalent surface electric current density $\mathbf{J}_\Omega$ and the magnetic current density $\mathbf{M}_\Omega$ [14]. The boundary condition is the tangential component of electromagnetic fields that are continuous at the boundary. The electric field integral equation is a summation for the electric field in external and internal regions as follows:

$$-\mathbf{E}^i(\boldsymbol{r})\hat{f}(s) = \hat{t}\cdot\sum_{m=1}^{2}\left[s\mu_0 L_m(\boldsymbol{r},\boldsymbol{r}')\cdot\mathbf{J}_\Omega(\boldsymbol{r}') + K_m(\boldsymbol{r},\boldsymbol{r}')\cdot\mathbf{M}_\Omega(\boldsymbol{r}')\right]. \tag{1}$$

Similarly, the magnetic field integral equation is expressed as

$$-\mathbf{H}^i(\boldsymbol{r})\hat{f}(s) = \hat{t}\cdot\sum_{m=1}^{2}\left[K_m(\boldsymbol{r},\boldsymbol{r}')\cdot\mathbf{J}_\Omega(\boldsymbol{r}') + \frac{s\mu_0}{\eta_m^2}L_m(\boldsymbol{r},\boldsymbol{r}')\cdot\mathbf{M}_\Omega(\boldsymbol{r}')\right] \tag{2}$$

where $\hat{t}$ is a unit tangential vector on the boundary, and L_m and K_m are integral operators defined by

$$L_m(\boldsymbol{r},\boldsymbol{r}')\cdot\mathbf{X}(\boldsymbol{r}') = \int_\Omega\left[\mathbf{X}(\boldsymbol{r}') - \frac{\nabla\nabla}{S_m^2}\mathbf{X}(\boldsymbol{r}')\right]g_m(\boldsymbol{r},\boldsymbol{r}')\,d\Omega' \tag{3}$$

$$K_m(\boldsymbol{r},\boldsymbol{r}')\cdot\mathbf{X}(\boldsymbol{r}') = \int_\Omega \mathbf{X}(\boldsymbol{r}')\times\nabla g_m(\boldsymbol{r},\boldsymbol{r}')\,d\Omega' \tag{4}$$

$$g_m(\boldsymbol{r},\boldsymbol{r}') = \frac{\exp\left(-S_m^2|\boldsymbol{r}-\boldsymbol{r}'|\right)}{4\pi|\boldsymbol{r}-\boldsymbol{r}'|} \tag{5}$$

where η_m is wave impedance and $S_m = s(\varepsilon_m\mu_m)^{-1}$. The unknown functions are electric current density $\mathbf{J}_\Omega$ and magnetic current density $\mathbf{M}_{\Omega,}$, and are discretized by basis function [12]. These can be obtained by solving a linear equation based on (1) and (2). Here, when the scatterer is the complex multimaterials composite objects, definition of the basis function is a cumbersome procedure. In this case, it is necessary to consider using that another integral equation method should be considered [19]. Electromagnetic fields in the complex frequency domain are computed by the unknown functions. The solution for the complex frequency domain $F(s)$ obtained by PMCHWT is transformed into the time-domain by FILT [11]–[13]. Using the approximate exponential function and residual theorem, the time-domain function $f(t)$ is expressed by

$$f(t) := \frac{\exp(\alpha)}{t}\sum_{n=1}^{K}(-1)^n\mathrm{Im}\left[F(s_n)\right] \tag{6}$$

where t is the observation time, α is the approximation parameter, K is the truncation number, and s_n is the sampling complex frequency as defined by

$$s_n = \frac{\alpha + i(n-0.5)\pi}{t}. \tag{7}$$

III. Computational Results

To verify our proposed method, we investigated the electric field near a gold nano sphere with a 25 nm radius. The observation point is at 30 nm on the x-axis. The incident wave is assumed to be a sinusoidal plane wave and has only electric field of x component. The incident angles are $\theta_{\text{in}} = \phi_{\text{in}} = 0°$. Fig. 2 shows the time domain responses of the electric field at

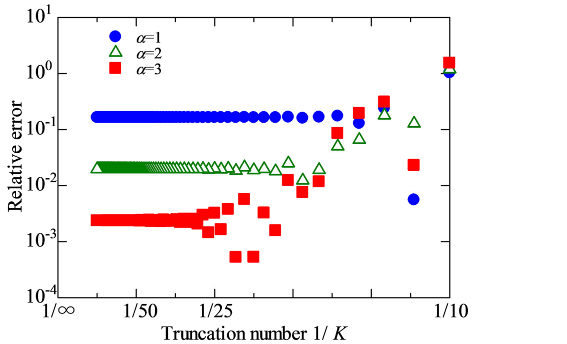

Fig. 3. Convergence process of the relative error for varying truncation numbers. The relative error is defined by the difference between the computational value and the exact one.

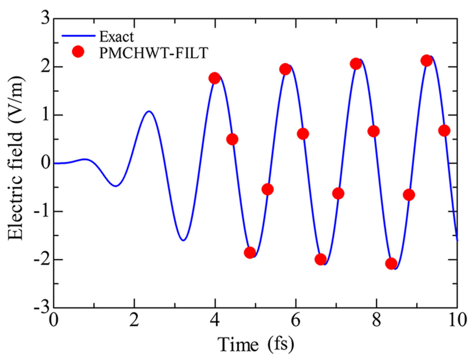

Fig. 4. Time domain response for relatively large time step size.

the observation point. Red X's indicate the computational results obtained by our method, and the blue line indicates the exact Mie series solution [12]. The computational results correspond to the exact solution for all points in time.

The convergence process shows the relative error for varying the truncation number of FILT K as shown in Fig. 3. The relative error is defined by the difference between the computational value and the Mie series solution at $t = 9.25$ fs [12]. The error converges by increasing the truncation number K and the converged value depends on the selection of the approximation parameter α. If $\alpha = 1$ and $K > 25$, the relative error converges to 10^{-1}. It tends to 10^{-3} order when $\alpha = 3$ and $K > 50$. The proposed method can precisely control the computational accuracy by selecting the approximation parameter α and proper truncation number K for which the converged value is obtained.

Fig. 4 shows the time response for the relatively large step size of one-quarter period. Compared with the time step size of FDTD with a minimum cell size of 1 nm, our time step size is over 200 times. For large intervals, the computational results obtained by our method and the exact solution are a good match. With our method, the electromagnetic field at the desired observation time can be obtained.

To compare the FDTD method, the electric field near a gold nano spheroid is investigated as shown in Fig. 5. The observation point is at 45 nm on the x-axis and the incident wavelength is 550 nm. In Fig. 6, all computational results are in complete agreement. The time step size of our method was selected about 40 times that of the FDTD. The memory requirement of the FDTD was 16 GB and that of our method was about 1 GB.

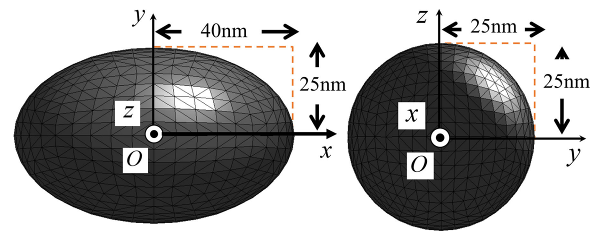

Fig. 5. Computational model for the spheroid.

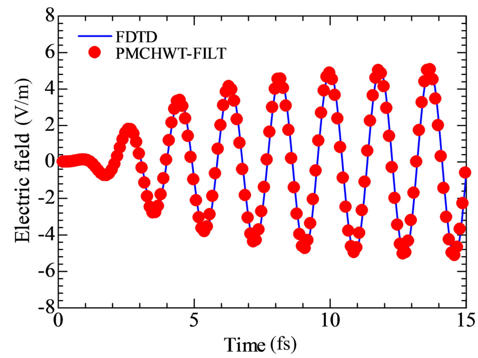

Fig. 6. Time response of electric field for the nano spheroid.

TABLE I
SPEED UP RATE FOR TIME-DIVISION PARALLEL COMPUTING

Number of computers	Speed up rate
1	1
2	1.9997
5	4.9983
10	9.9926

We can perform a time-division and complete parallel computing which has the advantage in efficiency. The speed up rate is verified in Table I. In our method, the computational task can be divided into multi computers. The speed up rate always corresponds to the number of computers, since there is no data communication.

The application of our proposed method is discussed here, and the plasmonic device for a helicity-dependent all-optical magnetic switching has been designed. In this system, the localized circular light is required for ultra-high-speed, high density recording. To obtain the localized circular polarized light, a cross-bar type antenna is assumed, and has been designed using gold as the material. To produce the phase difference between the x- and y-components of the electric fields for circular polarized light, the characteristics of the cross-bar based antenna investigated in Fig. 7. The incident light is assumed to be a linearly polarized sinusoidal plane wave. The incident angles are $\theta_{\rm in} = \phi_{\rm in} = 0°$. The amplitude of the electric field is 1 V/m and the wavelength is 780 nm. The observation point is at the center of the antenna.

Fig. 8 shows the electric field and phase shift for varying lengths in the x-direction. The length of the y direction bar is fixed. The phase shifts are based on the phase at x-length $=$ 49 nm, which is the peak of the electric field. To generate the circularly polarized light from linearly polarized light, a 90° phase difference is necessary. The lengths of bars for the x- and y-directions are selected to be 42 and 51 nm, respectively,

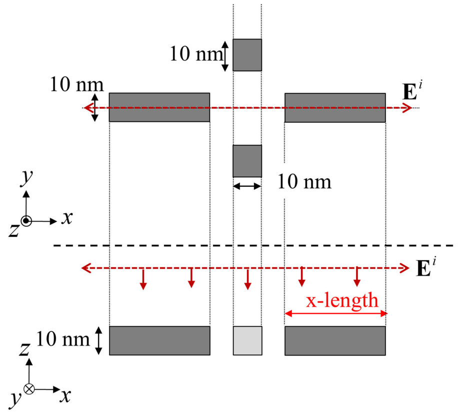

Fig. 7. Computational model for designing a cross-bar type antenna.

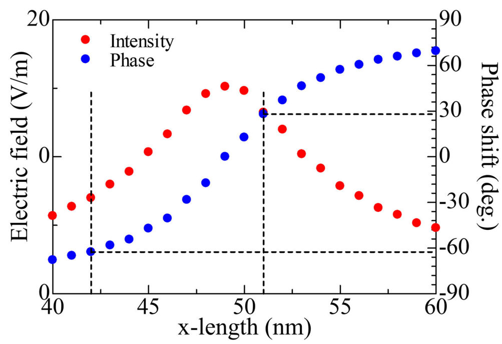

Fig. 8. Electric field and phase shift for varying x-length, which is the length of the bars in the x-direction.

because those values produce a 90° phase shift. Here, to match the amplitude of the electric field intensity of the x- and y-components, the incident angle becomes $\phi_{\mathrm{in}} = 61.2°$.

To confirm that this antenna can generate the localized circular polarized light, electric field intensity and circularity distribution are shown in Fig. 9(a) and (b), respectively. The electric field is enhanced around the center of the device. The clockwise circularly polarized light is generated from linearly polarized light.

Moreover, the transient analysis is important for evaluation of the generation time of circular polarized light, and is related to the recording speed. Our method is suitable for these problems, because small time increments are not required to evaluate the transient response time. Fig. 10(a) and (b) shows the time response and the Lissajous curve of the electric field at the center of the device using our method. We can confirm that the x- and y-components of the electric field are uniform in steady state after $t = 30$ fs. The generation of clockwise circularly polarized light from a linearly polarized light has been successfully demonstrated.

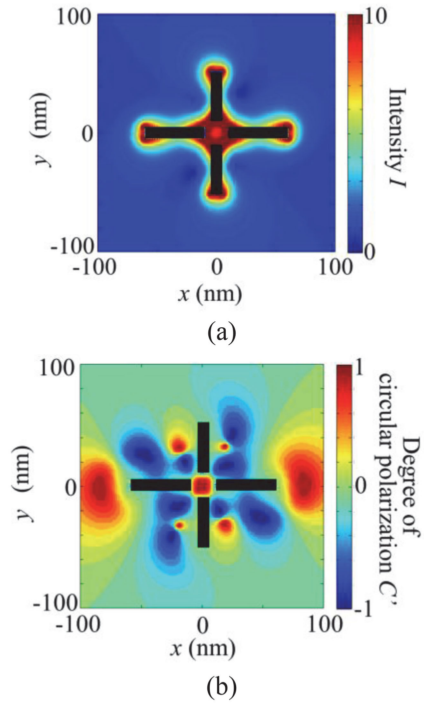

Fig. 9. Evaluation of field distribution. (a) Electric field intensity and (b) circularity distribution.

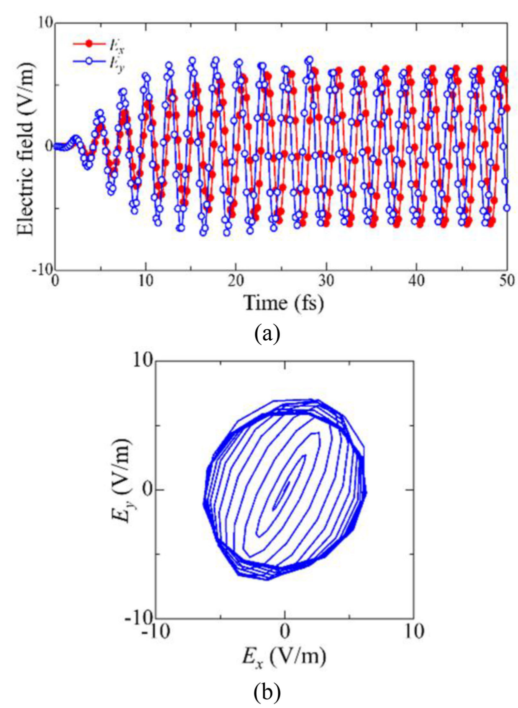

Fig. 10. Evaluation of electric fields at the center of the antenna. (a) Time-domain response and (b) Lissajous figure.

IV. Conclusion

In this letter, we propose a novel computational technique for time domain analysis of plasmonic devices. FILT is applied for PMCHWT formulation in the complex frequency domain. Some advantages of our method include the following: dispersive media such as the metal for light band can be easily considered, and computational error can be easily controlled, and the electromagnetic field at desired observation time can be obtained. Finally, the application of our method was demonstrated. The plasmonic antenna that generates the localized circular polarized light can be designed and evaluated in terms of transient state.

REFERENCES

[1] C. D. Stanciu *et al.*, "All-optical magnetic recording with circularly polarized light," *Phys. Rev. Lett.*, vol. 99, pp. 047601–1–047601–4, 2007.

[2] C.-H. Lambert *et al.*, "All-optical control of ferromagnetic thin films and nanostructures," *Science*, vol. 345, pp. 1337–1340, 2014.

[3] S. Mangin *et al.*, "Engineered materials for all-optical helicity-dependent magnetic switching," *Nature Mater.*, vol. 13, pp. 286–292, 2014.

[4] K. Nakagawa, Y. Ashizawa, S. Ohnuki, A. Itoh, and A. Tsukamoto, "Confined circularly polarized light generated by nano-size aperture for high density all-optical magnetic recording," *J. Appl. Phys.*, vol. 109, no. 7, pp. 07B735–1–07B735–3, 2011.

[5] B. Koene, M. Savoini, A. V. Kimel, A. Kirilyuk, and T. Rasing, "Optical energy optimization at the nanoscale by near-field interference," *Appl. Phys. Lett.*, vol. 101, no. 1, pp. 013115–1–013115–4, 2012.

[6] S. Y. Huang, W. C. Chew, Y. G. Liu, B.-I. Wu, and H. W. Choi, "A pancake-shaped nano-aggregate for focusing surface plasmons," *J. Appl. Phys.*, vol. 111, no. 3, pp. 034308–1–034308–5, 2012.

[7] A. Taflove and S. C. Hagness, *Computational Electrodynamics*, 2nd ed. Norwood, MA, USA: Artech House, 1995.

[8] D. Wu, R. Ohnishi, R. Uemura, T. Yamaguchi, and S. Ohnuki, "Finite-difference complex-frequency-domain method for optical and plasmonic analyses," *IEEE Photon. Technol. Lett.*, vol. 30, no. 11, pp. 1024–1027, Jun. 2018.

[9] S. Ohnuki, R. Ohnishi, D. Wu, and T. Yamaguchi, "Time-division parallel FDTD algorithm," *IEEE Photon. Technol. Lett.*, vol. 30, no. 24, pp. 2143–2146, Dec. 2018.

[10] D. Wu, S. Kishimoto, and S. Ohnuki, "Optimal parallel algorithm of fast inverse laplace transform for electromagnetic analyses," *IEEE Antennas Wireless Propag. Lett.*, vol. 19, no. 12, pp. 2018–2022, Dec. 2020.

[11] T. Hosono, "Numerical inversion of laplace transform and some applications to wave optics," *Radio Sci.*, vol. 16, no. 6, pp. 1015–1019, 1981.

[12] S. Masuda, S. Kishimoto, and S. Ohnuki, "Reference solutions for time domain electromagnetic solvers," *IEEE Access*, vol. 8, no. 1, pp. 44318–44324, 2020.

[13] S. Kishimoto, S. Nishino, and S. Ohnuki, "Novel computational technique for time-dependent heat transfer analysis using fast inverse Laplace transform," *Prog. Electromagn. Res. M*, vol. 99, pp. 45–55, 2021.

[14] W. C. Chew, M. S. Tong, and B. Hu, *Integral Equation Methods For Electromagnetic and Elastic Waves*. San Rafael, CA, USA: Morgan & Claypool, 2009.

[15] I. E. Uysal, H. A. Ülkü, and H. Bağcı, "MOT solution of the PMCHWT equation for analyzing transient scattering from conductive dielectrics," *IEEE Antennas Wireless Propag. Lett.*, vol. 14, pp. 507–510, 2014.

[16] I. E. Uysal, H. A. Ülkü, and H. Bağci, "Transient analysis of electromagnetic wave interactions on plasmonic nanostructures using a surface integral equation solver," *J. Opt. Soc. Amer.*, vol. 33, no. 9, pp. 1747–1759, 2016.

[17] W. H. Press, S. A. Teukolsky, W. T. Vetterling, and B. P. Flannery, *Numerical Recipes in C*, 2nd ed. New York, NY, USA: Cambridge Univ. Press, 1992.

[18] A. D. Rakic, A. B. Djurisic, J. M. Elazar, and M. L. Majewski, "Optical properties of metallic films for vertical-cavity optoelectronic devices," *Appl. Opt.*, vol. 37, no. 22, pp. 5271–5283, 1998.

[19] R. Zhao, Y. Chen, X. M. Gu, Z. Huang, H. Bagci, and J. Hu, "A local coupling multitrace domain decomposition method for electromagnetic scattering from multilayered dielectric objects," *IEEE Trans. Antennas Propag.*, vol. 68, no. 10, pp. 7099–7108, Oct. 2020.